20

Optimization of H4 Parallel Manipulator Using Genetic Algorithm

M. Falahian, H.M. Daniali* and S.M. Varedi
Babol University of Technology
Iran

1. Introduction

Parallel manipulators have the advantages of high stiffness and low inertia compared to serial ones (Merlet, 2006). Most pick-and-place operations, including picking, packing and palletizing tasks; require four-degree-of-freedom (DOF), i.e. three translations and one rotation around a vertical axis (Company et al, 2003). A new family of 4-DOF parallel manipulator being called H4 that could be useful for high-speed, pick-and-place applications is proposed by Pierrot and Company (Pierrot & Company, 1999). This manipulator offers 3-DOF in translation and 1-DOF in rotation about a given axis. The H4 manipulator is useful for high-speed handling in robotics and milling in machine tool industry since it is a fully-parallel mechanism with no passive chain which can provide high performance in terms of speed and acceleration (Wu et al, 2006). Its prototype, built in the Robotics Department of LIRMM, can reach 10g accelerations and velocities higher than 5 m/s (Robotics Department of LIRMM). Pierrot et al. proved the efficiency of H4 serving as a high-speed pick-and-place robot (Pierrot et al, 2006). Corradini et al. evaluated the 4-DOFs parallel manipulator stiffness by two methods and compared the results (Coradini & Fauroux, 2003). Renaud et al. presented the kinematic calibration of a H4 robot using a vision-based measuring device (Renaud et al, 2003). Tantawiroon et al. designed and analyzed a new family of H4 parallel robots (Tantawiroon & Sangveraphunsiri, 2003). Poignet et al. estimated dynamic parameters of H4 with interval analysis (Poignet et al, 2003).

Parallel manipulators suffer from smaller workspaces relative to their serial counterparts; therefore, many researchers addressed the optimization of their workspaces (Boudreau & Gosselin, 1999; Laribi et al, 2007). But optimization for such a purpose might lead to a manipulator with poor dexterity. To alleviate this drawback some others considered both performance indices and volume of workspace, simultaneously (Li & Xu, 2006; Xu & Li, 2006; Lara et al, 2010).

This chapter deals with an optimal design of H4 parallel manipulator aimed at milling and Rapid-Prototyping applications with three degrees of freedom in translation and one in rotation. The forward and inverse kinematics of the manipulator are solved. The forward kinematics analysis of H4 leads to a univariate polynomial of degree eight. The workspace of the manipulator is parameterized using several design parameters. Some geometric constraints are considered in the problem, as well. Because of nonlinear discontinuous behaviour of the

* Corresponding Author

problem, Genetic Algorithm (GA) Method is used here to optimize the workspace. Finally, using GA, the manipulator is optimized based on a mixed performance index that is a weighted sum of global conditioning index and its workspace. It is shown that by introducing this measure, the parallel manipulator is improved at the cost of workspace reduction.

2. Description and mobility analysis of a H4 parallel manipulator

The basic concept of H4 is described by a simple architectural scheme as illustrated in Fig. 1, where joints are represented by lines (Pierrot et al, 2001). The manipulator is based on four independent chains between the base and the End-Effector (EE); each chain is driven by an actuator which is fixed on the base. Let P, R, U and S represent prismatic, revolute, universal, and spherical joints, respectively. Each of the *P-U-U* and *R-U-U* chains must satisfy some geometrical conditions to guarantee that the manipulator offers three translations and one rotation about a given axis (see (Pierrot & Company, 1999) for details). The *U-U* and $(S\text{-}S)_2$ (or $(U\text{-}S)_2$) chains can be considered as "equivalent" in terms of number and type of degrees of motion, so the *P-U-U* (or *R-U-U*) chains can be replaced by $P\text{-}(U\text{-}S)_2$ or $P\text{-}(S\text{-}S)_2$ chains (respectively by $R\text{-}(U\text{-}S)_2$ or $R\text{-}(S\text{-}S)_2$). In this chapter, $P\text{-}(S\text{-}S)_2$ chain is chosen for the mechanism architecture of H4. Fig. 2 shows the architecture of H4 (chain #1 is not plotted for sake of simplicity) (Poignet et al, 2010).

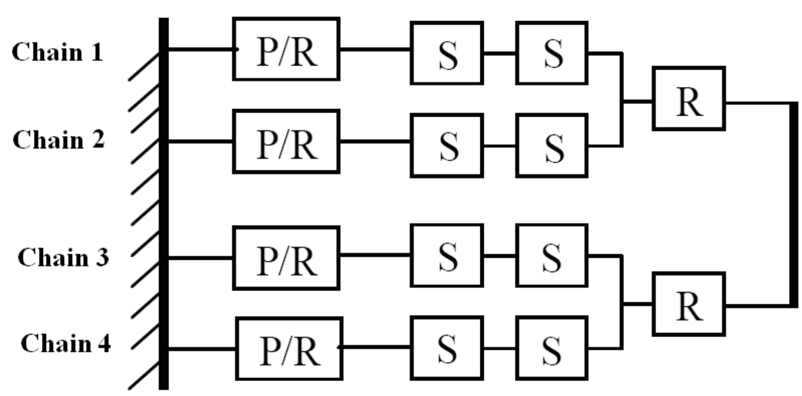

Fig. 1. Architectural scheme of H4

It is noteworthy that the four independent chains are not directly connected to the EE. It is possible to add another revolute joint on this end part and to couple it (with gears, timing belt, etc (Robotics Department of LIRMM)) so that the range of motion obtained on this latter joint can be larger than the end part ones. It is even possible to equip this passive revolute joint with a sensor to improve the robot accuracy. Moreover, the manipulator is a high-speed mechanism and can be easily controlled. So the H4 manipulator has the ability of serving as an efficient pick-and-place robot.

Considering the H4 robotic structure as given in Fig. 2, its geometrical parameters of are defined as follows:

- Two frames are defined, namely {A}: a reference frame fixed on the base; {B}: a coordinate frame fixed on the EE (C_1-C_1).
- The actuators slide along guide-ways oriented along a unitary vector, $\overrightarrow{k_z}$ ($\overrightarrow{k_z}$ is the unity vector parallel to the z axis in the reference frame {A}), and the origin is point $\mathbf{P_i}$, so the position of each point $\mathbf{A_i}$ is given by: $\vec{\mathbf{A}}_i = \vec{\mathbf{P}}_i + \mathbf{q}_i \vec{\mathbf{z}}_i$; for i=1,…4, in which $\mathbf{q_i}$ is the actuator coordinates.

- The parameters $\mathbf{M_i}$, d and h are the length of the rods, the offset of the revolute-joint from the ball-joint, and the offset of each ball-joint from the center of the traveling plate, respectively.
- The pose of the EE is defined by a position vector $\vec{\mathbf{B}} = \begin{bmatrix} x & y & z \end{bmatrix}^T$ and an angle θ, representing its orientation.

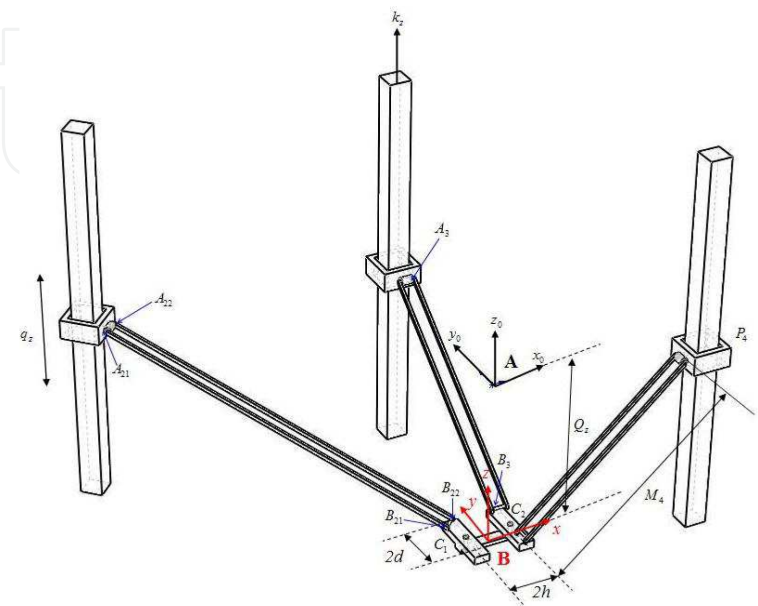

a) Robot with four lines drives and $(S-S)_2$ chains

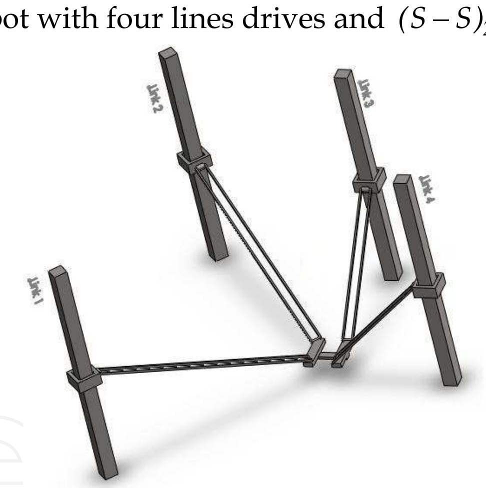

b) Robot CAD model

Fig. 2. H4 parallel manipulator

Without losing generality, in this chapter we consider $\vec{\mathbf{P}}_i = \begin{bmatrix} a_i & b_i & 0 \end{bmatrix}^T$ for simplicity, Q_z is the offset of {B} from {A} along the direction of $\overline{k_z}$.
One can effectively analyze the mobility of a H4 parallel manipulator by resorting to screw theory, which is a convenient tool to study instantaneous motion systems that include both rotation and translation in three dimensional spaces (Zhao et al, 2004).
A screw is called a twist when it is used to describe the motion state of a rigid body and a wrench when it is used to represent the force and moment of a rigid body. If a wrench acts on a rigid body in such a way that it produces no work, while the body is undergoing an infinitesimal twist, the two screws are said to be reciprocal (Li & Xu, 2007). In a parallel

manipulator, the reciprocal screws associated with a serial limb represent the wrench constraints imposed on the moving platform by the serial limb. The motions of the moving platform are determined by the combined effect of all the wrench constraints imposed by each limb. Therefore, we can get the following equation:

$$\$_r^T \circ \$ = 0 \tag{1}$$

where $\$_r$ is the reciprocal screw and "$\circ$" represents the reciprocal production of two screws (Dai & Jones, 2007). According to the physical interpretations of reciprocal screws, one can obtain the constraints spaces that should be spanned by all of the reciprocal screws. As far as a H4 parallel manipulator is concerned, each S joint is equivalent to three intersecting non-coplanar R joints, and then the joint twists associated with the ith *P-(S-S)₂-R* (or *P-U-U-R*) chain form a 6-system, which can be identified in the fixed frame as follows:

$$\begin{aligned} &\$_1^i = \begin{bmatrix} 0 \\ \vec{s}_1^i \end{bmatrix}, \quad \$_2^i = \begin{bmatrix} {}_1\vec{s}_{A_i}^i \\ A_i \times {}_1\vec{s}_{A_i}^i \end{bmatrix}, \quad \$_3^i = \begin{bmatrix} {}_2\vec{s}_{A_i}^i \\ A_i \times {}_2\vec{s}_{A_i}^i \end{bmatrix} \\ &\$_4^i = \begin{bmatrix} {}_1\vec{s}_{B_i}^i \\ B_i \times {}_1\vec{s}_{B_i}^i \end{bmatrix}, \quad \$_5^i = \begin{bmatrix} {}_2\vec{s}_{B_i}^i \\ B_i \times {}_2\vec{s}_{B_i}^i \end{bmatrix}, \quad \$_6^i = \begin{bmatrix} \vec{s}_{C_i}^i \\ C_i \times \vec{s}_{C_i}^i \end{bmatrix} \end{aligned} \tag{2}$$

where $\vec{s}_j^i$ denotes a unit vector along the jth joint axis of the ith chain, for $i = 1,...,4$. Therefore, the kinematic screws of each kinematic chain can be expressed as:

$$[\$^i]^T = \begin{bmatrix} \$_1^i & \$_2^i & \$_3^i & \$_4^i & \$_5^i & \$_6^i \end{bmatrix} \tag{3}$$

Therefore, the reciprocal screws of kinematic chains can be derived as:

$$[\$_{platform}^r]^T = \begin{bmatrix} \$_r^1 & \$_r^2 & \$_r^3 & \$_r^4 \end{bmatrix} \tag{4}$$

Finally one can compute null spaces of the foregoing reciprocal screws which leads to the DOF of the manipulator; namely,

$$\begin{aligned} DoF_1 &= \begin{bmatrix} 0 & 0 & 0 & 1 & 0 & 0 \end{bmatrix}^T \\ DoF_2 &= \begin{bmatrix} 0 & 0 & 0 & 0 & 1 & 0 \end{bmatrix}^T \\ DoF_3 &= \begin{bmatrix} 0 & 0 & 0 & 0 & 0 & 1 \end{bmatrix}^T \\ DoF_4 &= \begin{bmatrix} 0 & 0 & 1 & 0 & 0 & 0 \end{bmatrix}^T \end{aligned} \tag{5}$$

These imply that H4 robot has three translational and one rotational DOF. Figure 3 shows the rotation of C_1C_2 link about z-axis as rotational DOF.

3. Kinematic analysis

3.1 Inverse kinematics

The inverse position kinematics problem solves the actuated variables from a given pose of EE. Let $\mathbf{q} = \begin{bmatrix} q_1 & q_2 & q_3 & q_4 \end{bmatrix}^T$ be the array of the four actuator joint variables and

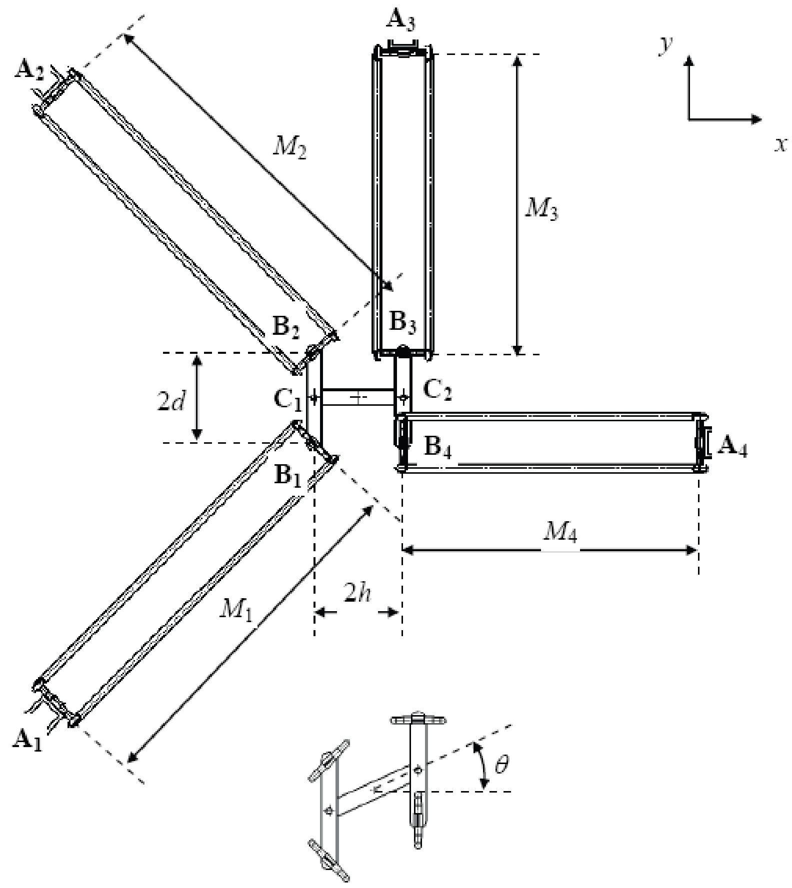

Fig. 3. Design parameters of H4

$\vec{\mathbf{x}} = [x \quad y \quad z \quad \theta]^T$ be the array of the pose of the EE. The position of points C_1 and C_2 are given by [4]:

$$\vec{\mathbf{C}}_1 = \vec{\mathbf{B}} + \mathrm{Rot}(\theta)\overrightarrow{\mathbf{BC_1}} \qquad \vec{\mathbf{C}}_2 = \vec{\mathbf{B}} + \mathrm{Rot}(\theta)\overrightarrow{\mathbf{BC}_2} \tag{6}$$

where $\mathbf{Rot}(\theta)$ denotes the rotation matrix of the EE with respect to reference frame and is defined as:

$$\begin{aligned}\mathbf{Rot}(\theta) &= {}^{A}\mathbf{R}_B = \mathbf{R}_z(\theta) \\ &= \begin{bmatrix} cos(\theta) & -sin(\theta) & 0 \\ sin(\theta) & cos(\theta) & 0 \\ 0 & 0 & 1 \end{bmatrix}\end{aligned} \tag{7}$$

Moreover, the position of each point $\mathbf{B_i}$ is given by:

$$\begin{aligned} \vec{\mathbf{B}}_1 &= \vec{\mathbf{C}}_1 + \overrightarrow{\mathbf{C}_1\mathbf{B}_1} \qquad & \vec{\mathbf{B}}_2 &= \vec{\mathbf{C}}_1 + \overrightarrow{\mathbf{C}_1\mathbf{B}_2} \\ \vec{\mathbf{B}}_3 &= \vec{\mathbf{C}}_2 + \overrightarrow{\mathbf{C}_2\mathbf{B}_3} \qquad & \vec{\mathbf{B}}_4 &= \vec{\mathbf{C}}_2 + \overrightarrow{\mathbf{C}_2\mathbf{B}_4} \end{aligned} \tag{8}$$

Therefore, the following can then be written:

$$||A_iB_i||^2 = M_i^2 \tag{9}$$

Then, for the first chain:

$$\begin{aligned}
&\overrightarrow{\mathbf{A}_1\mathbf{B}_1} = (\vec{\mathbf{B}} + \mathbf{Rot}(\theta)\overrightarrow{\mathbf{BC}}_1 + \overrightarrow{\mathbf{C}_1\mathbf{B}_1} - \vec{\mathbf{P}}_1) - q_1\vec{\mathbf{z}}_1 \\
&(A_1B_1)^2 = q_1^{\,2} - 2q_1 d_1.z_1 + \|d_1\|^2
\end{aligned} \tag{10}$$

where $\vec{\mathbf{d}}_1 = \vec{\mathbf{B}} + \mathbf{Rot}(\theta)\overrightarrow{\mathbf{BC}}_1 + \overrightarrow{\mathbf{C}_1\mathbf{B}_1} - \vec{\mathbf{P}}_1$. Finally, the two solutions of Eq. 10 are given by:

$$q_1 = \vec{\mathbf{d}}_1.\vec{\mathbf{z}}_1 \pm \sqrt{(\vec{\mathbf{d}}_1.\vec{\mathbf{z}}_1)^2 + M_1^{\,2} - \|\mathbf{d}_1\|^2} \tag{11}$$

Similarly, q_1, q_2 and q_4 can be derived as:

$$\begin{aligned}
&q_2 = \vec{\mathbf{d}}_2.\vec{\mathbf{z}}_2 \pm \sqrt{(\vec{\mathbf{d}}_2.\vec{\mathbf{z}}_2)^2 + M_2^{\,2} - \|\mathbf{d}_2\|^2} \qquad \vec{\mathbf{d}}_2 = \vec{\mathbf{B}} + \mathbf{Rot}(\theta)\overrightarrow{\mathbf{BC}}_1 + \overrightarrow{\mathbf{C}_1\mathbf{B}_2} - \vec{\mathbf{P}}_2 \\
&q_3 = \vec{\mathbf{d}}_3.\vec{\mathbf{z}}_3 \pm \sqrt{(\vec{\mathbf{d}}_3.\vec{\mathbf{z}}_3)^2 + M_3^{\,2} - \|\mathbf{d}_3\|^2} \qquad \vec{\mathbf{d}}_3 = \vec{\mathbf{B}} + \mathbf{Rot}(\theta)\overrightarrow{\mathbf{BC}}_2 + \overrightarrow{\mathbf{C}_2\mathbf{B}_3} - \vec{\mathbf{P}}_3 \\
&q_4 = \vec{\mathbf{d}}_4.\vec{\mathbf{z}}_4 \pm \sqrt{(\vec{\mathbf{d}}_4.\vec{\mathbf{z}}_4)^2 + M_4^{\,2} - \|\mathbf{d}_4\|^2} \qquad \vec{\mathbf{d}}_4 = \vec{\mathbf{B}} + \mathbf{Rot}(\theta)\overrightarrow{\mathbf{BC}}_2 + \overrightarrow{\mathbf{C}_2\mathbf{B}_4} - \vec{\mathbf{P}}_4
\end{aligned} \tag{12}$$

3.2 Forward kinematics

Forward kinematic problem solves the pose of the EE from a given actuators variables. It is well-known that forward kinematic problem of parallel manipulators is challenging (Dasgupta & Mruthyunjaya, 2000) and involves the solution of a system of nonlinear coupled algebraic equations in the variables describing the platform posture. This system of nonlinear equations might lead to solutions. Except in a limited number of the problems, one has difficulty in finding exact analytical solutions for the problem. So these nonlinear simultaneous equations should be solved using other methods, namely, numerical or semi-exact analytical methods. Some others believe that the combination of numerical and semi-exact analytical methods can also produce useful results (Hashemi et al, 2007; Varedi et al, 2009). Choi et al. solved forward kinematic problem of H4 and showed that the problem lead to a 16th degree polynomial in a single variable (Choi et al, 2003).

The EE is composed of three parts (two lateral bars and one central bar). Moreover, points $\mathbf{B}_1$, $\mathbf{B}_2$, $\mathbf{B}_3$ and $\mathbf{B}_4$ form a parallelogram. Let ${}^A\mathbf{A}_i$ and ${}^A\mathbf{B}_i$ represent the homogeneous coordinates of the points $\mathbf{A}_i$ in {A} and $\mathbf{B}_i$ in {A}, respectively. Then, one can write (Wu et al, 2006):

$$\begin{aligned}
&{}^A\vec{\mathbf{B}}_i = \begin{bmatrix} x + hE_{1i}\,c\theta \\ y + hE_{1i}\,s\theta + dE_{2i} \\ z \\ 1 \end{bmatrix} = \begin{bmatrix} P_i\,c\theta + x \\ P_i\,s\theta + y + Q_i \\ z \\ 1 \end{bmatrix} \\
&{}^A\vec{\mathbf{A}}_i = \begin{bmatrix} a_i & b_i & q_i & 1 \end{bmatrix}^T
\end{aligned} \tag{13}$$

where

$$\begin{aligned}
&P_i = hE_{1i},\ Q_i = dE_{2i},\ E_{11} = E_{12} = -1,\ E_{13} = E_{14} = -1, \\
&E_{21} = E_{24} = 1,\ E_{22} = E_{23} = 1,\ c\theta = cos(\theta),\ s\theta = sin(\theta)
\end{aligned} \tag{14}$$

Substituting these values in Eq.(9), upon simplifications, yields:

$$(P_i c\theta + x - a_i)^2 + (P_i s\theta + y + Q_i - b_i)^2 + (z - q_i)^2 = M_i^2 \quad i = 1,\dots,4 \tag{15}$$

Expanding and rearranging Eq.(15) leads to:

$$\begin{aligned}&\tilde{A}_i x + \tilde{B}_i y + \tilde{C}_i z + \tilde{D}_i + \tilde{E}_i = 0 \quad for \;\; i = 1,\dots,4\\&\tilde{A}_i = 2(P_i c\theta - a_i), \quad \tilde{B}_i = 2(P_i s\theta + Q_i - b_i) \quad \tilde{C}_i = -2q_i\\&\tilde{D}_i = a_i^2 + b_i^2 + q_i^2 - 2P_i(a_i c\theta + b_i s\theta - Q_i s\theta) - 2Q_i b_i + P_i^2 + Q_i^2 - M_i^2\\&\tilde{E}_i = x^2 + y^2 + z^2\end{aligned} \tag{16}$$

Subtracting Eq.(16) for i=3, 4 from the same equation for i=2, yields to:

$$\Delta A_{23} x + \Delta B_{23} y + \Delta C_{23} z + \Delta D_{23} = 0 \tag{17}$$

$$\Delta A_{24} x + \Delta B_{24} y + \Delta C_{24} z + \Delta D_{24} = 0 \tag{18}$$

where

$$\begin{aligned}&\Delta A_{23} = (\tilde{A}_2 - \tilde{A}_3), \Delta B_{23} = (\tilde{B}_2 - \tilde{B}_3), \Delta C_{23} = (\tilde{C}_2 - \tilde{C}_3), \Delta D_{23} = (\tilde{D}_2 - \tilde{D}_3),\\&\Delta A_{24} = (\tilde{A}_2 - \tilde{A}_4), \Delta B_{24} = (\tilde{B}_2 - \tilde{B}_4), \Delta C_{24} = (\tilde{C}_2 - \tilde{C}_4), \Delta D_{24} = (\tilde{D}_2 - \tilde{D}_4),\end{aligned}$$

Eqs. (17) and (18) now can be solved for x and y, namely:

$$x = \frac{\Delta_{11} z + \Delta_{12}}{\Delta_0} = e_1 z + e_2 \tag{19}$$

$$y = \frac{\Delta_{21} z + \Delta_{22}}{\Delta_0} = e_3 z + e_4 \tag{20}$$

where

$$\begin{aligned}&e_1 = \frac{\Delta_{11}}{\Delta_0}, e_2 = \frac{\Delta_{12}}{\Delta_0}, e_3 = \frac{\Delta_{21}}{\Delta_0}, e_4 = \frac{\Delta_{22}}{\Delta_0}, \;\; \Delta_0 = \Delta A_{23}\Delta B_{24} - \Delta A_{24}\Delta B_{23},\\&\Delta_{11} = \Delta B_{23}\Delta C_{24} - \Delta B_{24}\Delta C_{23}, \;\; \Delta_{12} = \Delta B_{23}\Delta D_{24} - \Delta B_{24}\Delta D_{23},\\&\Delta_{21} = \Delta A_{24}\Delta C_{23} - \Delta A_{23}\Delta C_{24}, \;\; \Delta_{22} = \Delta A_{24}\Delta D_{23} - \Delta A_{23}\Delta D_{24},\end{aligned}$$

Substituting Eqs.(19) and (20) into Eq.(16) for i=2, yields to the following quadratic equation.

$$\lambda_0 z^2 + \lambda_1 z + \lambda_2 = 0 \tag{21}$$

where

$$\begin{aligned}&\lambda_0 = e_1^2 + e_3^2 + 1, \quad \lambda_1 = 2e_1 e_2 + 2e_3 e_4 + \tilde{A}_2 e_1 + \tilde{B}_2 e_3 + \tilde{C}_2,\\&\lambda_2 = e_2^2 + e_4^2 + \tilde{A}_2 e_2 + \tilde{B}_2 e_4 + \tilde{D}_2\end{aligned}$$

Eq.(21) can be solved for z. Substituting this value into Eq.(16) for i=1, upon simplifications leads:

$$\begin{aligned}&f((c\theta)^4, (c\theta)^3(s\theta)^1, (c\theta)^2(s\theta)^2, (c\theta)^1(s\theta)^3, (c\theta)^0(s\theta)^4, (c\theta)^3(s\theta)^0,\\&(c\theta)^2(s\theta)^1, (c\theta)^1(s\theta)^2, (c\theta)^0(s\theta)^3, (c\theta)^2(s\theta)^0, (c\theta)^1(s\theta)^1, (c\theta)^0(s\theta)^2,\\&(c\theta)^1(s\theta)^0, (c\theta)^0(s\theta)^1, (c\theta)^0(s\theta)^0) = 0\end{aligned} \tag{22}$$

where f($x_1, x_2, ..., x_n$) represents a linear combination of $x_1, x_2, ..., x_n$. The coefficients of Eq.(22) are the data depend on the design parameters of the H4 robot. In Eq.(22), we substitute now the equivalent expressions for $c\theta$ and $s\theta$ given as:

$$c\theta = \frac{1-T^2}{1+T^2} \quad , \quad s\theta = \frac{2T}{1+T^2} \quad , \quad T = tan(\theta / 2) \tag{23}$$

Upon simplifications, Eq.(22) leads to a univariate polynomial of degree eight, namely;

$$aT^8 + bT^7 + cT^6 + dT^5 + eT^4 + fT^3 + gT^2 + hT^1 + i = 0 \tag{24}$$

where a, b, c, d, e, f, g, h and i depend on kinematic parameters. The detailed expressions for them are not given here because these expansions would be too large to serve any useful purpose. What is important to point out here is that the above equation admits eight solutions, whether real or complex, among which we only interested in the real ones. Substituting the values of T from Eq.(23) into Eq.(19), Eq.(20) and Eq.(21), complete the solutions.

3.2.1 Numerical example of kinematic analysis

Here, we include a numerical example as shown in Fig.4. The design parameters of H4 are given as:

$$h = d = 6\text{(cm)},\ Q_z = 42\text{(cm)}, M_1 = M_2 = \sqrt{3}Q_z, M_3 = M_4 = \sqrt{2}Q_z \tag{25}$$

Substituting these values in Eq.(13), yields:

$$\begin{aligned}
&\vec{\mathbf{A}}_1 = [-48 \quad -48 \quad 0]^T, \ \vec{\mathbf{B}}_1 = [-6 \quad -6 \quad -42]^T, \\
&\vec{\mathbf{A}}_2 = [-48 \quad 48 \quad 0]^T, \ \ \vec{\mathbf{B}}_2 = [-6 \quad 6 \quad -42]^T, \\
&\vec{\mathbf{A}}_3 = [6 \quad 48 \quad 0]^T, \quad \ \ \vec{\mathbf{B}}_3 = [6 \quad 6 \quad -42]^T, \\
&\vec{\mathbf{A}}_4 = [48 \quad -6 \quad 0]^T, \ \ \ \vec{\mathbf{B}}_4 = [6 \quad -6 \quad -42]^T.
\end{aligned}$$

Given, the position and orientation of the EE as $\vec{\mathbf{x}} = \begin{bmatrix} 5 & -5 & -30 & \pi / 6 \end{bmatrix}^T$, inverse kinematics are given by:

$$\vec{\mathbf{q}} = [13.021 \quad -7.488 \quad 9.679 \quad 15.77]^T \tag{26}$$

Next, the forward kinematic problem, for the actuators coordinate as given in Eq.(26), is solved. The polynomial equation in Eq.(24) can be solved for T, namely;

$$\begin{aligned}
&T_{12} = -0.61309 \pm 0.56609 i \\
&T_{34} = 0.073172 \pm 0.84245 i \\
&T_{56} = 0.028294 \pm 0.88575 i \\
&T_7 = 0.267957 \\
&T_8 = -2.8822
\end{aligned} \tag{27}$$

There are only two real solutions, for which $T_7 = 0.2680$ leads to $\vec{\mathbf{x}} = \begin{bmatrix} 5(cm) & -5(cm) & -30(cm) & 0.524(rad) \end{bmatrix}^T$ and $T_8 = -2.8822$, yields:

$\vec{\mathbf{x}} = \left[3(cm) \quad -7.95(cm) \quad -14.58(cm) \quad -2.47(rad)\right]^T$. However, the latter configuration cannot be realized in practice because of the mutual interference of the parallelograms as shown in Fig.4.

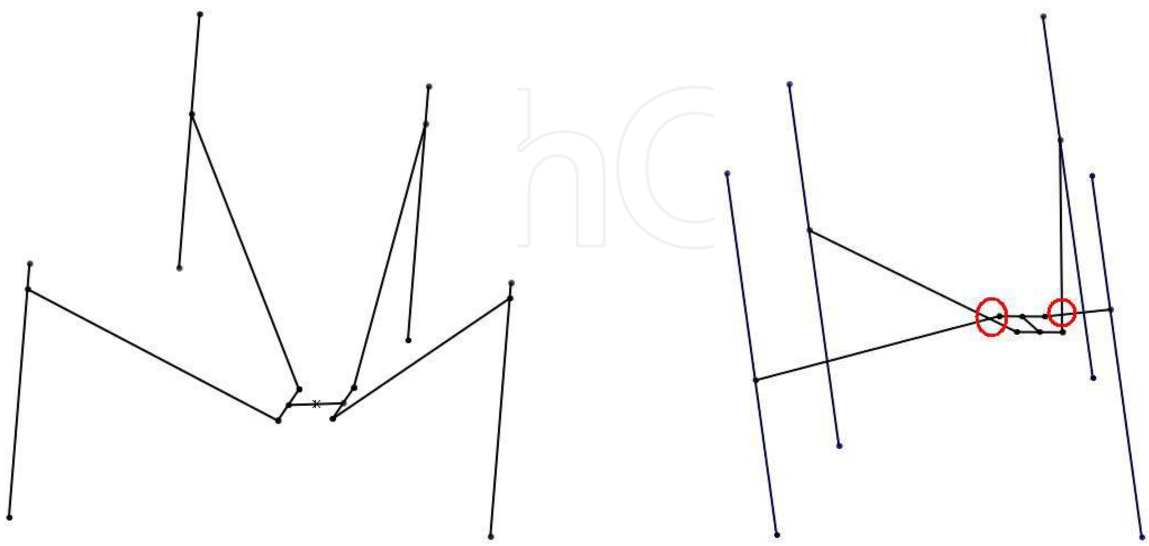

T_7 = 0.2680 T_8= - 2.8822

Fig. 4. The solutions for forward kinematic problem

3.3 Jacobian matrix

Jacobian matrix relates the actuated joint velocities to the EE Cartesian velocities, and is essential for the velocity and trajectory control of parallel robots. The velocity of the EE of H4 can be defined by resorting to a velocity for the translation, $\vec{\mathbf{v}}_B = \left[\dot{x} \quad \dot{y} \quad \dot{z}\right]^T$ and a scalar for the rotation about $\vec{\mathbf{z}}$; namely, $\dot{\theta}$. Thus, the velocity of points $C_1$and C_2 can be written as follows (Wu et al, 2006):

$$\vec{\mathbf{v}}_{c_1} = \vec{\mathbf{v}}_B + \dot{\theta}(\vec{\mathrm{k}}) \times \overrightarrow{\mathbf{BC}_1} \qquad \vec{\mathbf{v}}_{c_2} = \vec{\mathbf{v}}_B + \dot{\theta}(\vec{\mathrm{k}}) \times \overrightarrow{\mathbf{BC}_2} \tag{28}$$

Moreover, since the links $\mathbf{B}_1\mathbf{B}_2$ and $\mathbf{B}_3\mathbf{B}_4$ only have translational motion, the following relations hold:

$$\vec{\mathbf{v}}_{B_1} = \vec{\mathbf{v}}_{B_2} = \vec{\mathbf{v}}_{C_1} \qquad \vec{\mathbf{v}}_{B_3} = \vec{\mathbf{v}}_{B_4} = \vec{\mathbf{v}}_{C_2} \tag{29}$$

On the other hand, velocity of points A_i is given by:

$$\vec{\mathbf{v}}_{A_i} = \dot{q}\overrightarrow{k_z} \tag{30}$$

The velocity relationship can then be written thanks to the classical property; namely,

$$\vec{\mathbf{v}}_{A_i} \cdot \overrightarrow{\mathbf{A}_i\mathbf{B}_i} = \vec{\mathbf{v}}_{B_i} \cdot \overrightarrow{\mathbf{A}_i\mathbf{B}_i} \tag{31}$$

Eq.(31) can be written for i=1,…,4 and the results grouped in a matrix form as:

$$\mathbf{J}_q\dot{\vec{\mathbf{q}}} = \mathbf{J}_x\dot{\vec{\mathbf{x}}} \tag{32}$$

Where $\dot{\mathbf{x}}$ and $\dot{\mathbf{q}}$ denote the vectors of the EE velocity and input actuated joint rates, respectively ; $\mathbf{J}_q$ and $\mathbf{J}_x$ are the Jacobian matrices, all are defined as:

$$\dot{\mathbf{q}} = [\dot{q}_1 \quad \dot{q}_2 \quad \dot{q}_3 \quad \dot{q}_4]^T$$

$$\mathbf{J}_q = \begin{bmatrix} \overrightarrow{A_1B_1} \cdot \overrightarrow{\mathbf{z}_1} & 0 & 0 & 0 \\ 0 & \overrightarrow{A_2B_2} \cdot \overrightarrow{\mathbf{z}_2} & 0 & 0 \\ 0 & 0 & \overrightarrow{A_3B_3} \cdot \overrightarrow{\mathbf{z}_3} & 0 \\ 0 & 0 & 0 & \overrightarrow{A_4B_4} \cdot \overrightarrow{\mathbf{z}_4} \end{bmatrix}$$

$$\dot{\mathbf{x}} = [\dot{x} \quad \dot{y} \quad \dot{z} \quad \dot{\theta}]^T \tag{33}$$

$$\mathbf{J}_x = \begin{bmatrix} (\overrightarrow{A_1B_1})_x & (\overrightarrow{A_1B_1})_y & (\overrightarrow{A_1B_1})_z & (\overrightarrow{A_1B_1} \times \overrightarrow{BC_1}).\vec{\mathsf{k}} \\ (\overrightarrow{A_2B_2})_x & (\overrightarrow{A_2B_2})_y & (\overrightarrow{A_2B_2})_z & (\overrightarrow{A_2B_2} \times \overrightarrow{BC_1}).\vec{\mathsf{k}} \\ (\overrightarrow{A_3B_3})_x & (\overrightarrow{A_3B_3})_y & (\overrightarrow{A_3B_3})_z & (\overrightarrow{A_3B_3} \times \overrightarrow{BC_2}).\vec{\mathsf{k}} \\ (\overrightarrow{A_4B_4})_x & (\overrightarrow{A_4B_4})_y & (\overrightarrow{A_4B_4})_z & (\overrightarrow{A_4B_4} \times \overrightarrow{BC_2}).\vec{\mathsf{k}} \end{bmatrix}$$

If the mechanism is not in a singular configuration, the Jacobian and its inverse are described as:

$$\mathbf{J} = \mathbf{J}_x^{-1}\mathbf{J}_q \qquad and \qquad \mathbf{J}^{-1} = \mathbf{J}_q^{-1}\mathbf{J}_x \tag{34}$$

4. Optimization of H4

4.1 Workspace evaluation

For a robot in the context of industrial application and given parameters, it is very important to analyze the volume and the shape of its workspace (Dombre & Khalil, 2007). Calculation of the workspace and its boundaries with perfect precision is crucial, because they influence the dimensional design, the manipulator's positioning in the work environment, and its dexterity to execute tasks (Li & Xu, 2006). The workspace is limited by several conditions. The prime limitation is the boundary obtained through solving the inverse kinematic problem. Further, the workspace is limited by the reachable extent of drives and joints, then by the occurrence of singularities, and finally by the links and platform collisions (Stan et al, 2008). Various approaches may be used to calculate the workspace of a parallel robot. In the present work the boundary of workspace of H4 is determined geometrically (Merlet, 2006).

4.2 Condition number

In order to guarantee the regular workspace to be effective, constraints on the dexterity index are introduced into the design problem. A frequently used measure for dexterity of a manipulator is the inverse of the condition number of the kinematics Jacobian matrix (Hosseini et al, 2011). Indeed, in order to determine the condition number of the Jacobian matrices, their singular values must be ordered from largest to smallest. However, in the presence of positioning and orienting tasks the singular values associated with positioning, are dimensionless, while those associated with orientation have units of length, thereby making impossible such an ordering. This dimensional in-homogeneity can be resolved by introducing a weighting factor/length, which is here equal to the length of the first link (Hosseini et al, 2011). Then, the condition number of homogeneous Jacobian is defined as the ratio of its largest singular value σ_l to its smallest one, σ_s (Gosselin & Angeles, 1991), i.e.

$$\kappa(\mathbf{J}) \equiv \frac{\sigma_l}{\sigma_s} \tag{35}$$

Note that $\kappa(\mathbf{J})$ can attain any value from 1 to infinity, in which they correspond to isotropy and singularity, respectively.

4.3 Performance index

The objective function for maximization is defined here as a mixed performance index which is a weighted sum of global dexterity index (GDI), η_d and space utility ratio index (SURI), η_s (Dasgupta & Mruthyunjaya, 2000) , i.e.,

$$\begin{aligned} \eta &= w_d \eta_d + (1 - w_d)\eta_s \\ &= w_d \left[\frac{1}{V} \int_V \frac{1}{\kappa} dV \right] + (1 - w_d)\frac{V}{V^*} \end{aligned} \tag{36}$$

where the weight parameter $w_d \ (0 \le w_d \le 1)$ describes the proportion of GDI in the mixed index, and V^* represents the robot size which is evaluated by the product of area of the fixed platform and the maximum reach of the EE in the z direction.

4.4 Design variables

The architectural parameters of a H4 involve the offset of {B} from {A} along the direction of $\vec{k}_z(Q_z)$, length of the offset of the revolute-joint from the ball-joint (d) and the offset of each ball-joint from the center of the traveling plate (h). In order to perform the optimization independent of the dimension of each design candidate, the design variables are scaled by Δq, i.e., the motion range of the actuators. Thus, the design variables become $\vec{\Gamma} = \left[\frac{d}{\Delta q}, \frac{h}{\Delta q}, \frac{Q_z}{\Delta q} \right]$. However, we have the following limitations for the design variables:

$$1 / \kappa(\mathbf{J}) > 0.01,$$

$$0.01 < \frac{d}{\Delta q} < 0.15 \quad , \quad 0.01 < \frac{h}{\Delta q} < 0.15 \quad , \quad 0.35 < \frac{Q_z}{\Delta q} < 0.55$$

4.5 Optimization result of H4

In order to perform an optimal design of H4 parallel robots, an objective function was developed first, then GA is applied in order to optimize the objective function (Xu & Li, 2006). For optimization settings, regarding to the GA approach, normalized geometric selection is adopted (Merlet, 2006), and the genetic operators are chosen to be non-uniform mutation with the ratio of 0.08 and arithmetic crossover with the ratio of 0.8. Moreover, the population size is 30 and the generations' number is set to 150.

4.5.1 Optimization based on maximum workspace volume

First we consider the volume of workspace as the objective function; namely,

$V^{*}=max(V)$

Subject to

1. $1/\kappa(\mathbf{J}) > 0.01$

$$0.01 < \frac{d}{\Delta q} < 0.15 \quad , \quad 0.01 < \frac{h}{\Delta q} < 0.15 \quad , \quad 0.35 < \frac{Q_z}{\Delta q} < 0.55$$

The solution of this problem is given in Table 1. Moreover, the workspace for $\theta = 0$ and the conditioning index for $\theta = 0$ and z=0 are shown in Fig.5 and Fig.6, respectively. While the workspace size is acceptable, the manipulator suffers from a poor dexterity throughout its workspace.

Volume of workspace *(rad)(cm³)*	Average of conditioning index	Robot's parameters		
		d(cm)	*h(cm)*	Q_z *(cm)*
12582.0	0.042	13.52484	13.88781	35.18892

Table 1. Optimization result for H4

As it is observed the GA reaches a convergence after 30 iterations as depicted in Fig. 7.

4.5.2 Optimization based on GDI

In this section we optimize the average of conditioning index in the workspace. Therefore, the problem is stated as:

$GDI=\max(average\ (1/\ \kappa(\mathbf{J})\ ))$

Subject to

1. $1/\kappa(\mathbf{J}) > 0.01$
2. $0.01 < \frac{d}{\Delta q} < 0.15 \quad , \quad 0.01 < \frac{h}{\Delta q} < 0.15 \quad , \quad 0.35 < \frac{Q_z}{\Delta q} < 0.55$

As it is expected, the volume of the workspace is very small and only includes a small neighbourhood of a point of the best conditioning index. This optimal design is given in Table 2.

Volume of workspace *(rad)(cm³)*	Average of conditioning index	Robot's parameters		
		d(cm)	*h(cm)*	Q_z *(cm)*
4.1887	0.0705	1.00008	1.09692	35.48742

Table 2. Optimization result for H4

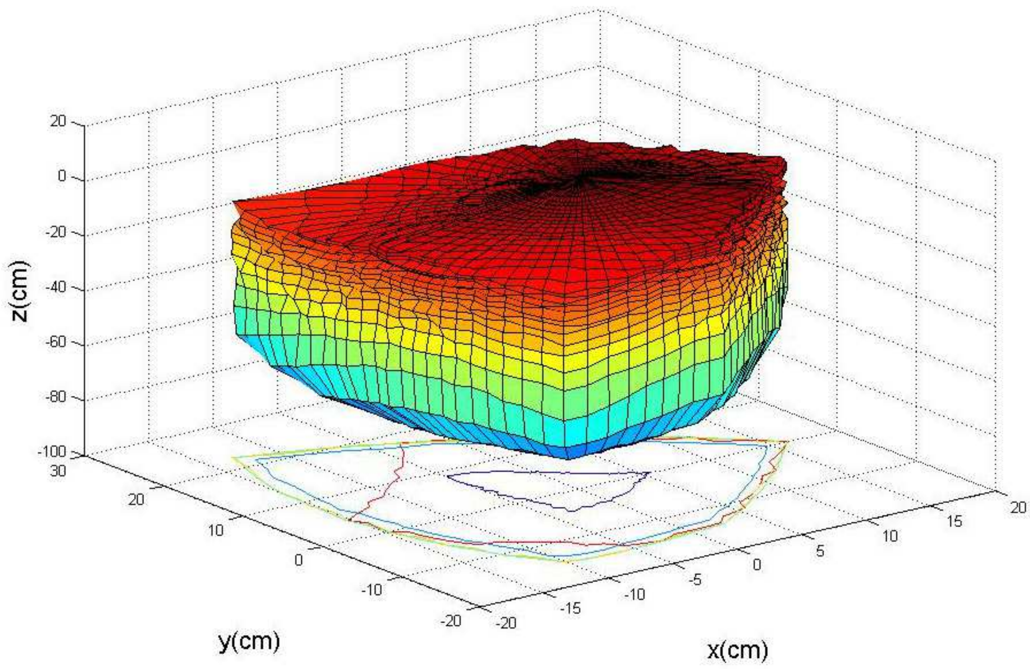

Fig. 5. Workspace of H4 for $\theta = 0$

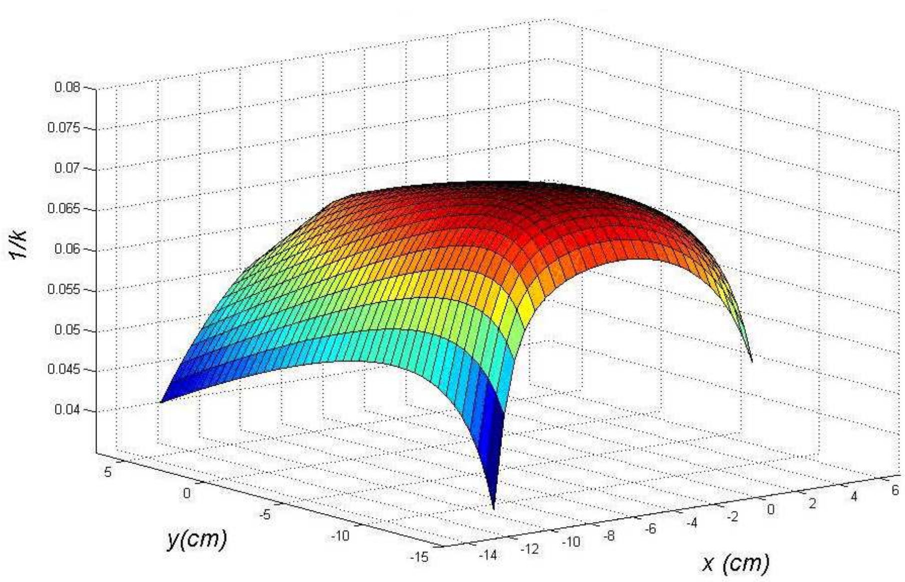

Fig. 6. Conditioning index for z=0 and $\theta = 0$

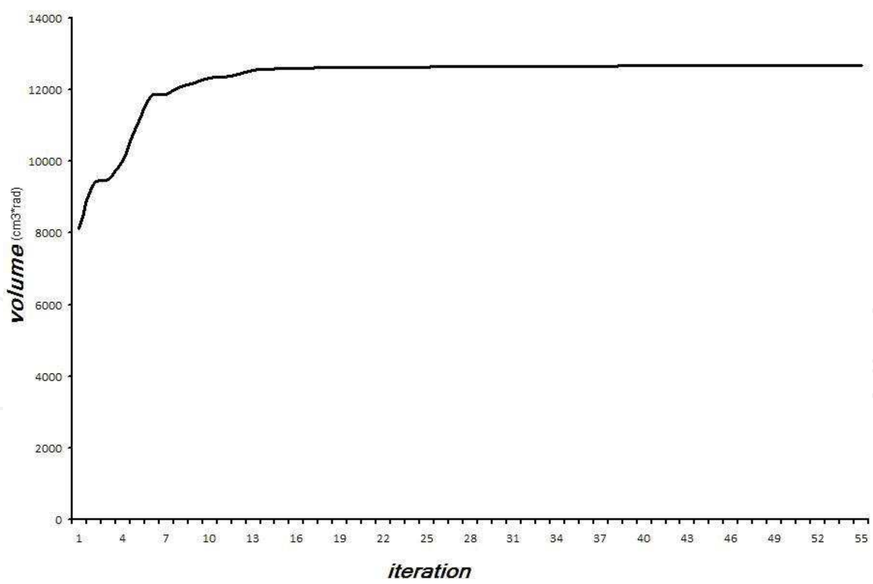

Fig. 7. Convergence of GA

4.5.3 Optimization based on the mixed performance index

For the problem at hand one needs a good fitness function, because the optimization based on maximal workspace volume, decreases the performance indices and the optimization based on GDI decreases the workspace volume. Therefore, one can optimize the manipulator based on performance index that described in subsection 5.3. The optimization results for w_d=0.25, 0.5, 0.75 are given in Table 3.

Moreover, for different values of w_d, the problem is solved and the GDI, SURI and the mixed performance index are calculated and plotted in Fig. 8. As the result, any value of w_d greater than 0.74 leads to a limited workspace and for any values smaller than that has no substantial effects on GDI and the workspace. Therefore, it clearly shows that by introducing this measure, the performance of the manipulator can be improved at a minor cost its workspace volume.

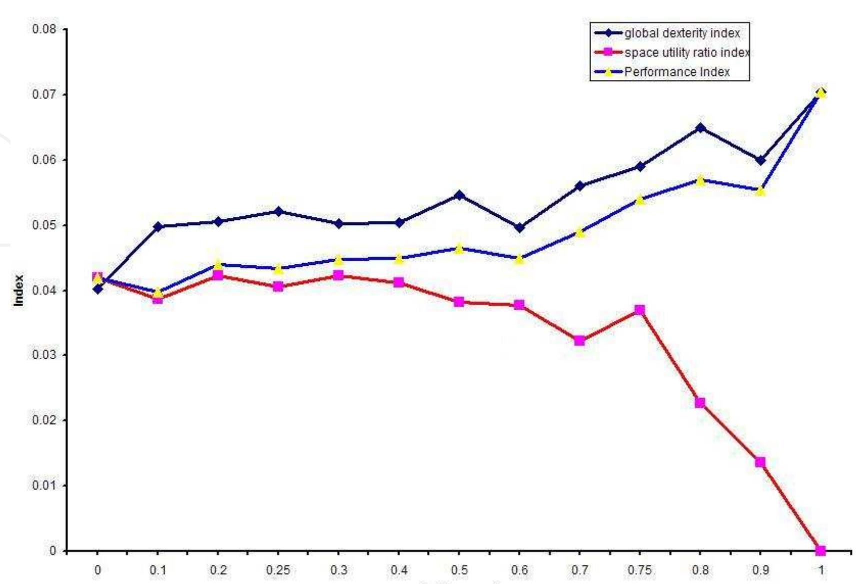

Fig. 8. GDI and SURI and Performance Index versus weight parameter

	$w_d = 0.25$	$w_d = 0.5$	$w_d = 0.75$
Volume of workspace *(rad)(cm³)*	11983	11304	11008
d(cm)	12.14243	12.60003	10.36257
h(cm)	10.38564	9.06147	5.56941
Q_z *(cm)*	37.25841	39.61105	40.69626
GDI	0.0521	0.0547	0.059

Table 3. Optimization results for H4

5. Conclusions

First, the forward and inverse kinematics of H4 parallel manipulator has been studied here, in which the former problem has leaded to a univariate polynomial of degree eight. Then, the optimal design of the manipulator has been addressed. Using genetic algorithm the manipulator has been optimized based on a mixed performance index that is a weighted sum of global conditioning index and its workspace volume. It has been shown that by introducing this measure, the parallel manipulator has been improved at minor cost of its workspace volume.

6. References

Boudreau, R.; Gosselin, C.M. (1999). The synthesis of planar parallel manipulators with a genetic algorithm, , *Journal of Mechanical Design*, 121(4), 1999, pp. 533–537.

Choi, H.B.; Konno, A. & Uchiyama, M. (2003). Closed-form solutions for the forward kinematics of a 4-DOFs parallel robot H4, *Proceedings of IEEE/RSJ International Conference on Intelligent Robots and Systems*, Las Vegas, USA, October, 2003, pp. 3312-3317.

Company, O.; Marquet, F. & Pierrot, F. (2003). A new high-speed 4DoF parallel robot synthesis and modeling issues. *IEEE, Transactions on Robotics and Automation*, Vol.19, No.3, 2003, pp. 411-420.

Coradini, C.; Fauroux, J. (2003). Evaluation of a 4-DOF parallel manipulator stiffness, *Mechanism and Machine Science*, Aug, 2003.

Dai, J.S.; Jones, J.R. (2007). A Linear Algebraic Procedure in Obtaining Reciprocal Screw Systems, *J. Robotic Systems*, 2007, 20(7), pp. 401–412.

Dasgupta, B.; Mruthyunjaya, T.S. (2000). The Stewart platform manipulator: A review, *Mechanism and Machine Theory*, 35, 2000, pp. 15–40.

Dombre, E.; Khalil, W. (2007). Modeling, Performance Analysis and Control of Robot Manipulators, *ISTE*, 2007.

Gosselin, C.; Angeles, J. (1991). A global performance index for the kinematic optimization of robotic manipulators. *ASME J Mech*, December, 1991, 113(3), pp. 220–226.

Hashemi, S.H.; Daniali, H.M. & Ganji, D.D. (2007). Numerical simulation of the generalized Huxley equation by He's homotopy perturbation method, *Applied Mathematics and Computation*, 2007, pp. 157–161.

Hosseini, M.A; Daniali, H.M. & Taghirad, H.D. (2011). "Dexterous Workspace Optimization of a Tricept Parallel Manipulator", *Advanced Robotics*, Vol. 25, 2011, pp. 1697-1712.

Lara-Molina, F.A.; Rosário, J.M. & Dumur, D. (2010). Multi-Objective Design of Parallel Manipulator Using Global Indices, *The Open Mechanical Engineering Journal*, 2010, 4, pp. 37-47.

Laribi, M.A.; Romdhane, L. & Zeghloul, S. (2007). Analysis and dimensional synthesis of the DELTA robot for a prescribed workspace, *Mechanism and Machine Theory*, 42, (2007), pp. 859–870.

Li, Yangmin.; Xu, Qingsong. (2006). A new approach to the architecture optimization of a general 3-PUU translational parallel manipulator. *J Int Robot System*, 2006, 46, pp. 59–72.

Li, Yangmin.; Xu, Qingsong. (2007). Kinematic analysis of a 3-PRS parallel manipulator, *Robotics and Computer-Integrated Manufacturing,* 2007, 23, pp. 395–408.

Merlet, J.P.; (2006). *Parallel robots* (second edition), springer.

Pierrot, F.; Company, O. (1999). H4: a new family of 4-DoF parallel robots, *Int Conf on Advanced Intelligent Mechatronics*, Proceedings of the 1999 IEEE/ASME, pp. 508-513.

Pierrot, F.; Marquet, F. & Company, O. & Gil, T. (2001). H4 parallel robot: modeling, design and preliminary experiments, *Int Conf on Robotics and Automation*, May, 2001.

Poignet, Ph.; Ramdani, N. & Vivas, O.A. (2003). Robust estimation of parallel robot dynamic parameters with interval analysis, *Proceedings of the 42nd IEEE*, Conference on Decision and Control, Maui, Hawaii USA, December, 2003.

Renaud, P.; Andreff, N. & Marquet, F. & Martinet, P. (2003). Vision-based kinematic calibration of a H4 parallel mechanism, *Int Conf on Robotics and Automation*, Proceediogr of the 2003 IEEE, Taipei, Taiwan, September 14-19.

Robotics Department of LIRMM. (n.d.). H4 with rotary drives: a member of H4 family, dedicated to high speed applications, http://www.lirmm.fr/w3rob.

Stan, S.D.; Manic, M. & Mătieş, M. & Bălan, R. (2008). Evolutionary approach to optimal design of 3 DOF Translation exoskeleton and medical parallel robots, *HSI 2008, IEEE Conference on Human System Interaction*, Krakow, Poland, May 25-27, 2008, pp. 720-725.

Tantawiroon, N.; Sangveraphunsiri, V. (2005). Design and analysis of a new H4 family parallel manipulator, *Thammasat Int J. Science Tech, July-September*, Vol. 10, No. 3, 2005.

Varedi, S.M.; Daniali, H.M. & Ganji, D.D. (2009). Kinematics of an offset 3-UPU translational parallel manipulator by the homotopy continuation method, *Nonlinear Analysis: Real World Applications 10*, 2009, pp. 1767–1774.

Wu, Jinbo.; Yin, Zhouping. & Xiong, Youlun. (2006). Singularity analysis of a novel 4-DoF parallel manipulator H4, *Int J Advanced Manuf Tech*, 29, pp. 794–802.

Xu, Qingsong.; Li, Yangmin. (2006). Kinematic analysis and optimization of a New compliant parallel micromanipulator, *Int J of Advanced Robotic Systems*, 2006, Vol. 3, No. 4.

Zhao, J.S.; Zhou, K. & Feng, Z.J. (2004). A theory of degrees of freedom for mechanisms. *Mechanism and Machine Theory*, 39, 2004, pp. 621–643.

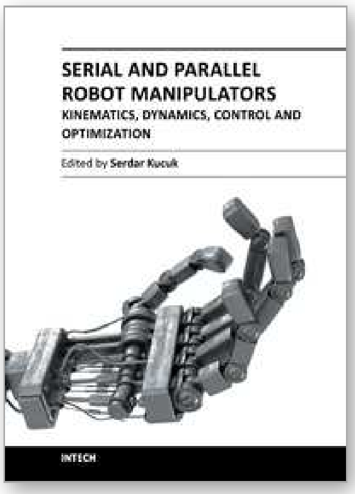

Serial and Parallel Robot Manipulators - Kinematics, Dynamics, Control and Optimization
Edited by Dr. Serdar Kucuk

ISBN 978-953-51-0437-7
Hard cover, 458 pages
Publisher InTech
Published online 30, March, 2012
Published in print edition March, 2012

The robotics is an important part of modern engineering and is related to a group of branches such as electric & electronics, computer, mathematics and mechanism design. The interest in robotics has been steadily increasing during the last decades. This concern has directly impacted the development of the novel theoretical research areas and products. This new book provides information about fundamental topics of serial and parallel manipulators such as kinematics & dynamics modeling, optimization, control algorithms and design strategies. I would like to thank all authors who have contributed the book chapters with their valuable novel ideas and current developments.